Energy Trapping and Detrapping in Reaction Center Mutants from *Rhodobacter sphaeroides*

Zivile Katiliene, Evaldas Katilius, and Neal W. Woodbury
Department of Chemistry and Biochemistry and the Center for the Study of Early Events in Photosynthesis, Arizona State University, Tempe, Arizona 85287-1604, USA

ABSTRACT Time-resolved fluorescence of chromatophores isolated from strains of *Rhodobacter sphaeroides* containing light harvesting complex I (LHI) and reaction center (RC) (no light harvesting complex II) was measured at several temperatures between 295 K and 10 K. Measurements were performed to investigate energy trapping from LHI to the RC in RC mutants that have a P/P^+ midpoint potential either above or below wild-type (WT). Six different strains were investigated: WT + LHI, four mutants with altered RC P/P^+ midpoint potentials, and an LHI-only strain. In the mutants with the highest P/P^+ midpoint potentials, the electron transfer rate decreases significantly, and at low temperatures it is possible to directly observe energy transfer from LHI to the RC by detecting the fluorescence kinetics from both complexes. In all mutants, fluorescence kinetics are multiexponential. To explain this, RC + LHI fluorescence kinetics were analyzed using target analysis in which specific kinetic models were compared. The kinetics at all temperatures can be well described with a model which accounts for the energy transfer between LHI and the RC and also includes the relaxation of the charge separated state $P^+H_A^-$, created in the RC as a result of the primary charge separation.

INTRODUCTION

The purple nonsulfur bacterium *Rhodobacter (Rb.) sphaeroides* has two different antenna complexes associated with its photosynthetic apparatus: Light harvesting complex II (LHII) and light harvesting complex I (LHI). LHII is a peripheral antenna system while LHI is in direct contact with the reaction center (RC). Excitation of LHII results in excitation energy transfer to LHI followed by energy transfer to the reaction center initial electron donor, P (a pair of bacteriochlorophyll molecules)(van Amerongen et al., 2000). In reaction centers, electron transfer then occurs from the first excited singlet state, P*, via bacteriochlorophyll B_A to bacteriopheophytin H_A in 3 ps at room temperature and 1 ps at 10 K, forming the state $P^+H_A^-$. The secondary electron transfer from H_A to the primary ubiquinone acceptor (Q_A) takes place in 200 ps and later to the secondary ubiquinone acceptor (Q_B) in 200 μs (Hoff and Deisenhofer, 1997; Kirmaier and Holten, 1987, 1993; Parson, 1996; Woodbury and Allen, 1995).

The energy transfer process from LHI to the reaction center has been investigated in several different species of purple bacteria. The energy transfer time in all species is ~35–40 ps at temperatures from 77 K to 295 K, and is the rate limiting step of the overall energy transfer and conversion process (Beekman et al., 1994; Bergstrom et al., 1989; Freiberg, 1995; Freiberg et al., 1996; Sundstrom et al., 1986; Timpmann et al., 1993; van Amerongen et al., 2000; Visscher et al., 1989; Xiao et al., 1994; Zhang et al., 1992).

One of the studies that provided evidence for the rate limiting role of the energy transfer step from LHI to the RC was performed using a series of RC mutants with altered P/P^+ midpoint potentials (Freiberg et al., 1996). These RC mutants have decreased rate constants for initial electron transfer (Allen and Williams, 1995). Only a weak dependence of the energy trapping time on the primary charge separation rate constant in the RC was observed, as would be expected if the energy transfer from LHI to the reaction center was the rate limiting step. However, the complete kinetic picture of the energy and electron transfer processes in these mutants was not established because it was not possible to directly observe the formation and decay of P* corresponding to energy transfer from the antenna to P and subsequent charge separation. The population of P* in the reaction center was too small at any particular time during the energy trapping process to be detected under the conditions used in this study. This was even true for a reaction center mutant in which the initial electron transfer rate constant was sevenfold slower than in wild-type. In addition, the spectral overlap of antenna and reaction center absorbance and fluorescence bands at room temperature made it difficult to distinguish between LHI and P* fluorescence (Freiberg et al., 1996; Xiao et al., 1994).

In this study, we revisit the energy trapping and detrapping process in membranes containing LHI complexes with reaction centers that have altered P/P^+ midpoint potentials. An expanded set of mutants covering a larger range of midpoint potentials is used. The measurements are performed as a function of temperature. This has made it possible to directly observe the fluorescence from both the LHI antenna excited state and P*, facilitating the development of kinetic models for the overall energy and electron transfer processes.

Submitted April 22, 2002, and accepted for publication January 14, 2003.

Address reprint requests to Zivile Katiliene, Fax: 480-965-2747; E-mail: zivile@asu.edu.

0006-3495/03/05/3240/12 $2.00

MATERIALS AND METHODS

Mutants

Time-resolved fluorescence spectroscopy was used to investigate energy trapping and detrapping in chromatophores of *Rb. sphaeroides* expressing

LHI and either wild-type or mutant reaction centers from a pRK plasmid in a background strain lacking functional LHI, LHII, and reaction center genes. Five reaction center mutants: HF(L168) + LHI (His changed to Phe at position L168) with a P/P^+ midpoint potential of 410 meV; LH(L131) + LHI (Leu to His at L131) with a P/P^+ midpoint potential of 585 meV; LH (L131) + LH(M160) + LHI (Leu to His at M160 + Leu to His at L131) with a P/P^+ midpoint potential of 635 meV; LH(L131) + LH(M160) + FH(M197) + LHI (Leu to His at M160 + Leu to His at L131 + Phe to His at M197) with a P/P^+ midpoint potential of 765 meV; WT + LHI with a P/P^+ midpoint potential of 505 meV, and the LHI-only strain without reaction centers were investigated at room and low temperatures (Williams et al., 1992; Mattioli et al., 1995; Woodbury et al., 1995). Reaction center mutants expressed in the LHI-only strain were constructed in *Rb. sphaeroides* as described previously (Allen and Williams, 1995; Freiberg et al., 1996; Williams et al., 1992). Chromatophores containing the mutated reaction centers and LHI were isolated as in (Freiberg et al., 1996). For room-temperature measurements, samples were suspended in TEN buffer (50 mM Tris-HCl (pH 8.0), 1 mM EDTA (pH 8.0), and 100 mM NaCl). For low-temperature measurements, samples were suspended in a (2:1 v/v) mixture of glycerol and TEN buffer. 10 mM sodium dithionite was added to each sample to reduce the quinone acceptors in the reaction center. The optical density of the samples was 0.1 at 875 nm in 2-mm pathlength for low temperature measurements and in 1-cm pathlength for room temperature measurements. A closed-circulation helium cryostat (APD Cryogenics Inc, Allentown, PA) was used to control sample temperature, as described previously (Williams et al., 1992).

Time-correlated single-photon counting

Energy transfer was investigated by measuring fluorescence kinetics using time-correlated single-photon counting (Lakowicz, 1999). The samples were excited with vertically polarized 860-nm light from a picosecond mode-locked titanium sapphire laser (Tsunami, Spectra Physics, Menlo Park, CA, pulse width <2 ps, repetition rate was 4 MHz using a Pulse Selector, Model 3980). The fluorescence was collected through a polarizer that was set at the magic angle relative to the vertical polarization of the excitation beam. Then fluorescence was passed through a double grating monochromator with a 4-nm spectral bandwidth and was detected by a S1-type microchannel plate photomultiplier tube (Hamamatsu Corporation, Bridgewater, NJ). The associated timing electronics have been described previously (Gust et al., 1990; Peloquin et al., 1994). The excitation intensity was ~50–100 $\mu W/cm^2$. At this intensity, no more than 1% of the antenna complexes in the sample were excited per pulse. The instrument response function was determined by measuring scattered light from a suspension of Ludox AS-40 (Sigma) at room temperature, and from the sample itself at 10–100 K. The full width at half maximum of the instrument response function was 50–70 ps. The fluorescence decay kinetics were measured every 10 nm from 880 to 960 nm at four temperatures: 10 K, 50 K, 100 K, and 294 K. Data were analyzed by global fitting of the fluorescence kinetics at each different temperature to a sum of exponential functions convoluted with the instrument response function using a data analysis program written locally in Matlab (Mathworks Inc, Natick, MA). Two, three, or four exponential functions were used, depending upon the sample and temperature, as required to achieve fits with a reduced χ^2 between 1.0 and 1.1. The error in determining each fitting parameter in this way was <10% as estimated by analyzing many measurements of the WT + LHI sample, with the exception of the first lifetime, which accuracy was limited by the width of the instrument response function. The kinetic traces were acquired to at least 10,000 counts in the maximum, although the number of counts varied for each fluorescence decay wavelength in the data set.

Data were also analyzed by target analysis (see Discussion), using a program written with Matlab software. The quality of the fits was evaluated by monitoring the residuals (difference between the fitting function and the actual data) for systematic deviations and by the value of the reduced χ^2, which varied from 1.0 to 1.1 in all mutants (indicating that the model used in the fitting accurately reproduced the data to within the limits of the noise), except in the double mutant, for which it was somewhat worse, 1.3–1.4. With the exception of the very fast rate constant describing initial electron transfer in the reaction center, the parameters resulting from the target analysis were determined with <10% error (variation of the parameters by >10% from their best fit values resulted in χ^2 increase to ~1.5–2). Accuracy in determination of the initial rate constant for electron transfer in the reaction center was less than that for the other target analysis parameters both because of the width of the instrument response function and because initial electron transfer was effectively convolved with the slower energy transfer reactions.

RESULTS

The fluorescence kinetics of the mutant photosynthetic membranes were measured at various wavelengths, covering the whole fluorescence spectrum, at four temperatures between 10 K and 294 K. Global fitting methods were used to analyze the data (Holzwarth, 1996). The lifetimes and decay-associated spectra (DAS) resulting from the global fits of the 10 K and room temperature data are shown in Figs. 1–6. The results obtained at 50 K and 100 K temperatures are available as supplementary data (see Supplementary Material).

The LHI-only mutant was fitted with two exponential decays at all temperatures (Fig. 1). The first component has a lifetime of ~230 ps and maximum initial amplitude that is ~17% of the total initial amplitude at 10 K. As the temperature is increased, this amplitude increases until it is ~50% at room temperature. The longer LHI fluorescence decay has a lifetime of 840 ps at 10 K and, at room temperature, the lifetime shortens slightly to 780 ps.

Fluorescence kinetics of WT + LHI and the LH(L131) + LHI mutant (P/P^+ midpoint 80 mV above WT) were fitted with four exponential decays at all temperatures. The decay-associated spectra of all components are very similar in both strains at low and room temperatures, except that the two longest components are more prominent in the LH(L131) + LHI (see Figs. 2 and 3). The decay-associated spectra for HF(L168) + LHI (P/P^+ midpoint potential 95 mV below WT) are shown in Fig. 4. Fluorescence kinetics of this low P/P^+ midpoint potential mutant were fitted with three exponential decays at low temperatures, and with four exponentials at room temperature. Again, the decay-associated spectra of all components are very similar to WT + LHI at any particular temperature, except that the longest component is not present at low temperatures and its amplitude is greatly reduced at room temperature compared to WT + LHI.

LH(L131) + LH(M160) + LHI (double mutant, 130 mV P/P^+ midpoint potential increase) and LH(L131) + LH (M160) + FH(M197) + LHI (triple mutant, 260 mV P/P^+ midpoint potential increase) fluorescence kinetics at all temperatures were fitted with three exponential decays; the decay-associated spectra are shown in Figs. 5 and 6, respectively. The low temperature decay-associated spectra for these mutants are strikingly different than those observed for the lower potential mutants. The most prominent difference

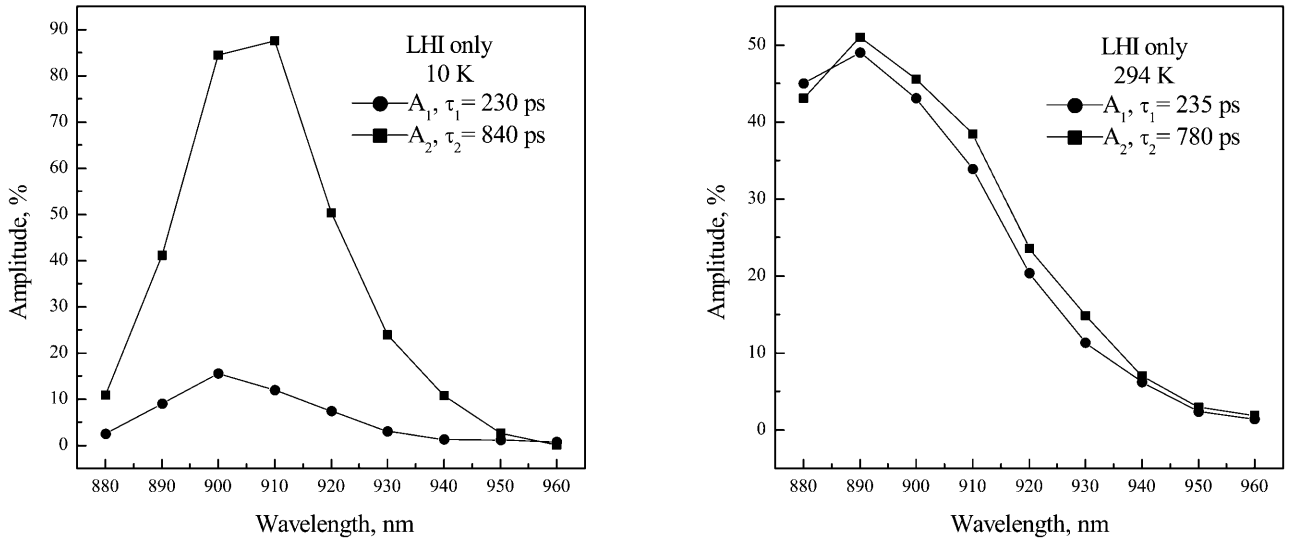

FIGURE 1 Decay-associated spectra resulting from fits of the fluorescence decay kinetics from chromatophores containing Light Harvesting Antenna I (LHI) only (no LHII or reaction centers) at 10 K and 294 K.

is the crossover of the first component spectrum from positive values to slightly negative values at long wavelengths, indicating energy transfer from LHI to RC. In each mutant, the decay-associated spectra of the second component are red-shifted compared to the spectra of the other components. In the case of the triple mutant, the spectrum of the second component corresponds almost entirely to fluorescence from P*. The second component from the double mutant shows a mixture of LHI and RC fluorescence, probably as a result of some equilibration between charge-separated and excited states. The spectrum of the longest component in each of the high potential mutants at 10 K is also slightly different from that of the other three mutants. In the double mutant its shape is similar to the spectrum of the second component, whereas in the triple mutant, the spectrum of the third component corresponds closely to the spectrum of LHI only. It is interesting to note that although at room temperature no crossover of the first component from positive to negative values can be resolved, the spectra of the second component in both double and triple mutants show fluorescence from P* in addition to that from the antenna (notice the increased intensity of the long wavelength fluorescence in the second component spectra compared with the first component in Figs. 5 and 6).

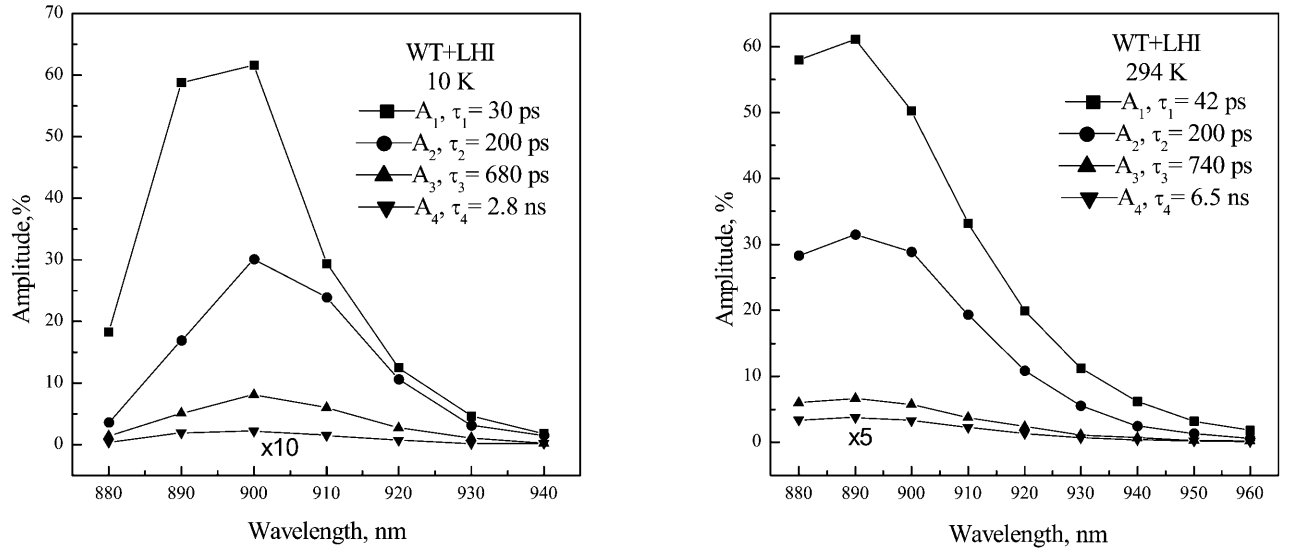

FIGURE 2 Decay-associated spectra resulting from fits of the fluorescence decay kinetics from chromatophores containing LHI and wild-type reaction centers (P/P^+ midpoint potential of 505 mV) at 10 K and 294 K. The amplitudes of the fourth component are multiplied by 10 at 10 K and by 5 at 294 K.

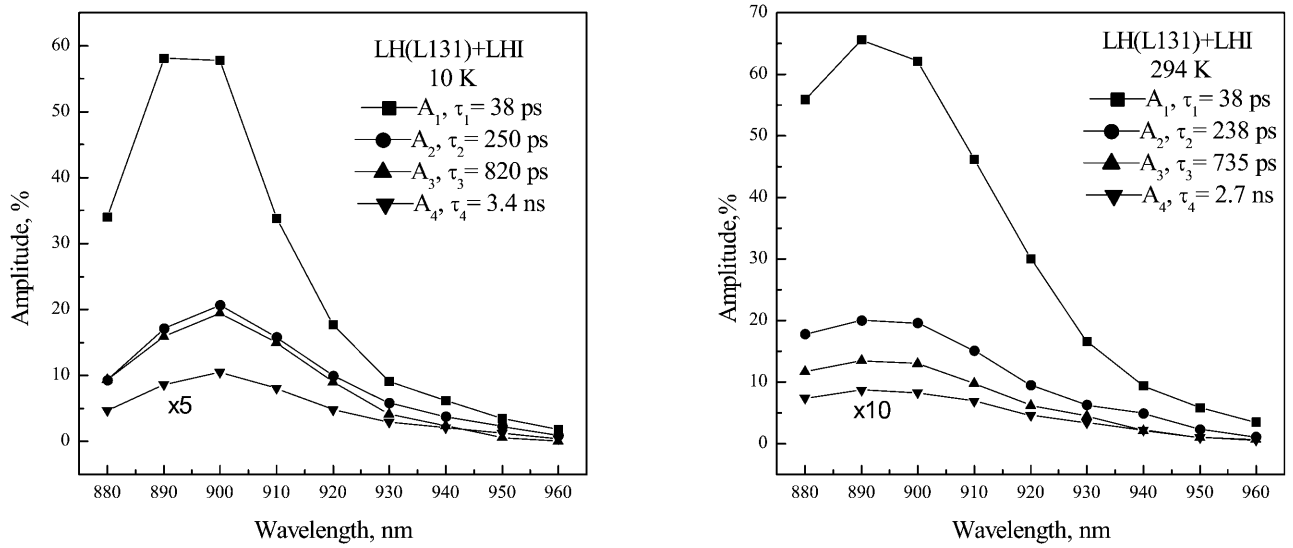

FIGURE 3 Decay-associated spectra resulting from fits of the fluorescence decay kinetics from chromatophores containing LHI/RC complexes with LH(L131) mutant reaction centers (P/P^+ midpoint potential of 585 mV) at 10 K and 294 K. The amplitudes of the fourth component are multiplied by 5 at 10 K and by 10 at 294 K.

DISCUSSION

Fluorescence decay of the LHI antenna alone

Structural studies of LHI complexes suggest that the LHI antenna complex in *Rb. sphaeroides* consists of a ring of $\alpha\beta$-subunit heterodimers that, between them, bind 32 bacteriochlorophylls (Walz et al., 1998), though there is still some discussion about whether the ring is complete or partially open (Frese et al., 2000; Vermeglio and Joliot, 1999). Previously, the fluorescence lifetime of detergent-isolated LHI complexes, not associated with functional reaction centers, was measured to be 680 ps at room temperature (Monshouwer et al., 1997). However, it was noted that the fluorescence lifetime was strongly dependent on aggregation of the sample and, in the membrane fragments, a shorter component of ~300 ps was found (Hunter et al., 1990; Monshouwer et al., 1997). As shown in Fig. 1, the excited state of the LHI antenna in the native membranes does not decay as a single exponential. At all temperatures, the fluorescence decay of the LHI-only mutant requires two exponential decay components for an adequate fit. The first component has a lifetime of ~230 ps at 10 K and 235 ps at

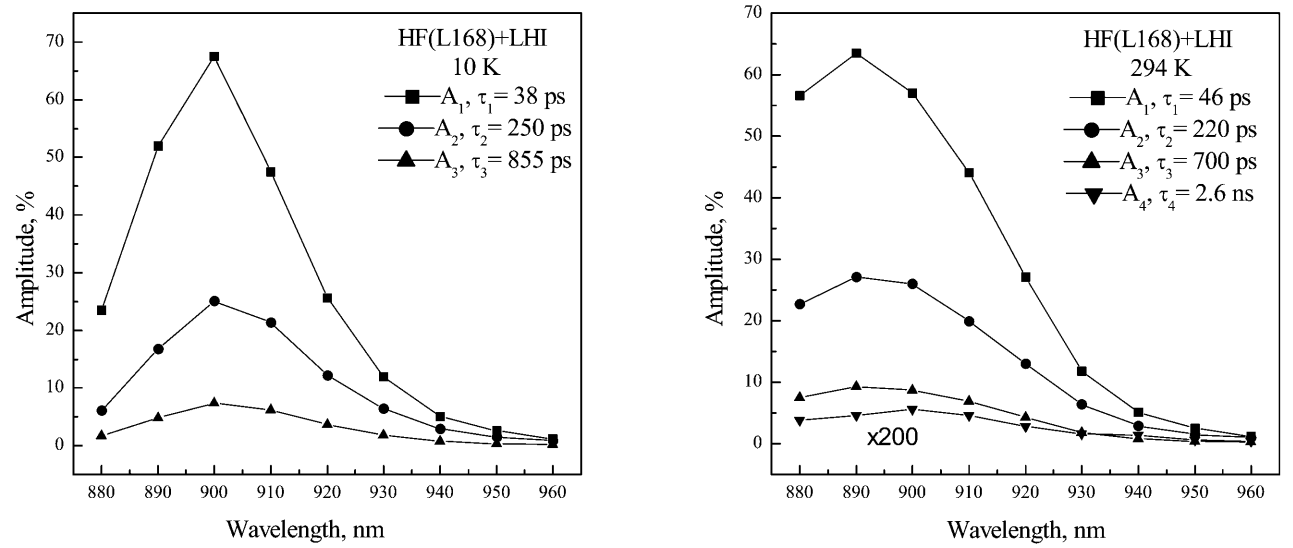

FIGURE 4 Decay-associated spectra resulting from fits of the fluorescence decay kinetics from chromatophores containing LHI/RC complexes with HF(L168) mutant reaction centers (P/P^+ midpoint potential of 410 mV) at 10 K and 294 K. The amplitude of the fourth component is multiplied by 200 at 294 K.

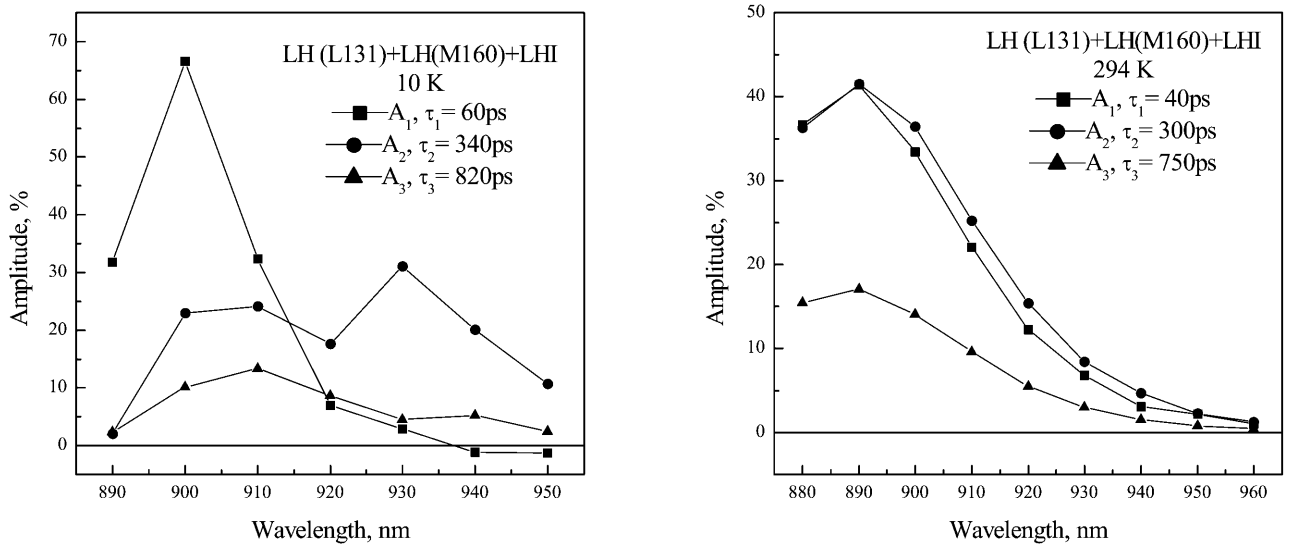

FIGURE 5 Decay-associated spectra resulting from fits of the fluorescence decay kinetics from chromatophores containing LHI/RC complexes with LH(L131) + LH(M160) mutant reaction centers (P/P^+ midpoint potential of 635 mV) at 10 K and 294 K.

294 K. The second component's lifetime is ~840 ps at 10 K and 780 ps at 294 K. In comparison to the isolated LHI complexes, one can assign the longer component as the intrinsic LHI fluorescence decay. The relative amplitudes of the two components are temperature dependent (Fig. 1). One possible explanation of this is that the first component may represent fluorescence due to LHI that is quenched by defects (''traps'') in the antenna (an oxidized antenna bacteriochlorophyll, for example). The amplitude of this component decreases with decreasing temperature suggesting that, at low temperature, energetic barriers caused by site inhomogeneity in the antenna restrict the movement of the excitations within the antenna and thus the accessibility of traps that quench fluorescence.

Energy transfer from LHI to the RC

The most striking finding of this report is that the rise in P* fluorescence, due to energy transfer from the excited state of LHI, can be directly observed in the high P/P^+ midpoint potential mutants LH(L131) + LH(M160) + LHI and LH(L131) + LH(M160) + FH(M197) + LHI at low temperatures (see Figs. 5 and 6 for 10 K and room temperature DAS, and Supplemental Material for 50 K and 100 K DAS.)

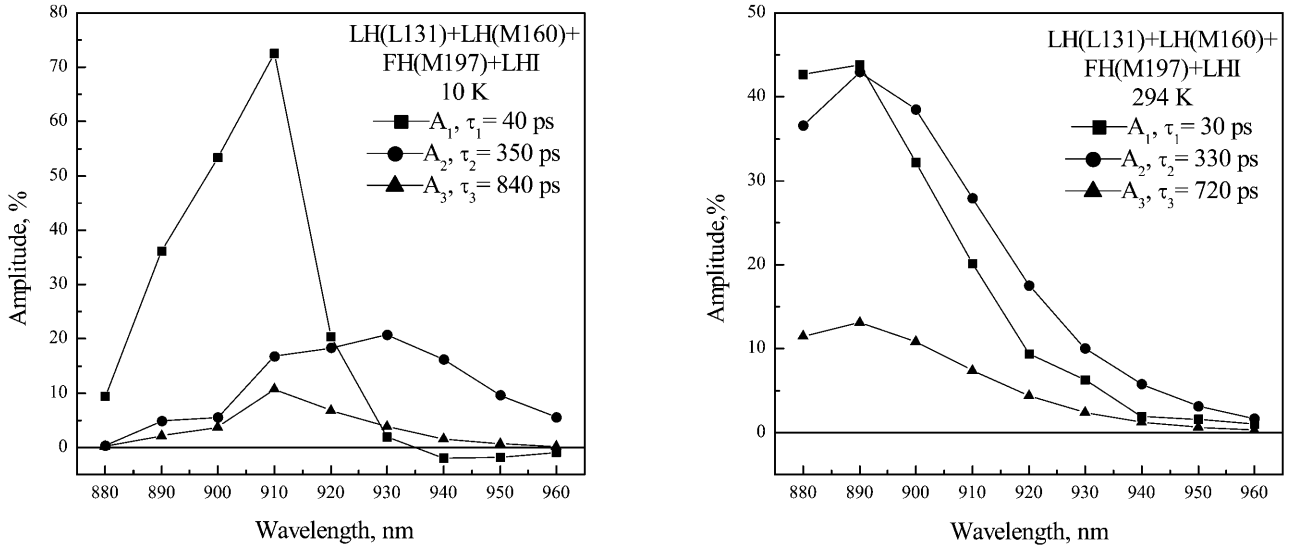

FIGURE 6 Decay-associated spectra resulting from fits of the fluorescence decay kinetics from chromatophores containing LHI/RC complexes with LH(L131) + LH(M160) + FH(M197) mutant reaction centers (P/P^+ midpoint potential of 765 mV) at 10 K and 294 K.

In these mutants, the P/P^+ midpoint potential is increased relative to wild-type by 160 mV and 260 mV, respectively. Thus, one might expect that the free energy of the state $P^+H_A^-$ will be shifted upwards toward P* by approximately the same amount, making P* and $P^+H_A^-$ almost isoenergetic in the triple mutant (Woodbury et al., 1995). The change in energetics is reflected in the primary electron transfer rate, which slows down from 3.5 ps in WT to roughly 25 ps in the double and 52 ps in the triple mutant at room temperature (Peloquin et al., 1994; Woodbury et al., 1995). At low temperatures, P* decay in the double mutant becomes kinetically heterogeneous, with P* decay components on several timescales including one ~40 ps and one >100 ps (Woodbury et al., 1994). In the triple mutant at low temperature, P* decay can be adequately fitted with a single lifetime of 290 ps (Woodbury et al., 1995). In both of these mutants, at low temperature, there are electron transfer yield losses, therefore the electron transfer time constant is slower than the measured P* decay time.

As the electron transfer rate slows down, the fluorescence quantum yield of P* in these mutants increases significantly compared to WT RCs. As a result, it is possible to directly detect the fluorescence from P* and resolve it kinetically, particularly at low temperature, since the rate of the energy transfer from LHI to the RC does not change significantly with temperature (Freiberg, 1995; Bergstrom et al., 1989). This can be seen in the decay-associated spectra of the double and triple mutants at 10 K (see Figs. 5 and 6). The spectra of the fastest component in each case changes from positive values below 930 nm (decay of the antenna fluorescence) to negative values at wavelengths >930 nm (rise of fluorescence from P*). The fact that the amplitude associated with the rise in P* fluorescence is much smaller than the amplitude associated with the decay of the antenna fluorescence (compare amplitudes at 900 nm and 950 nm in the 10 K spectrum of Figs. 5 and 6) implies that the yield of fluorescence from P*, in the double and triple mutant reaction centers, is lower than that from the excited state of the antenna. In addition, the overlap of the LHI and RC fluorescence spectra makes the rise in P* fluorescence difficult to observe because the strong positive LHI fluorescence decay component overlies the weaker negative fluorescence rise component from P* over much of the spectrum. At room temperature the negative rise component from P* is not resolved anymore (see Figs. 5 and 6), both because the P* fluorescence yield is lower at room temperature (electron transfer in these mutants is faster at room temperature) and also because the fluorescence spectra of LHI and P* broaden and overlap more at room temperature.

The second decay component of the double and triple mutants at 10 K has a lifetime of 340 ps and 350 ps, respectively. This component represents the subsequent decay of the fluorescence from LHI and P* in the case of the double mutant, and mostly of P* in the case of the triple mutant. This decay component most likely also represents equilibration of P* and $P^+H_A^-$. The spectrum of the second component at 10 K has maximum near 930 nm in both mutants (Figs. 5 and 6), as would be expected for P* (Woodbury and Allen, 1995). The longest component has a lifetime of ~800 ps, however, the spectral shapes of this component are somewhat different in the two mutants. In the double mutant, the spectrum of the third component is similar to the spectrum of the second component, suggesting that the third component likely includes fluorescence due to the charge recombination in the double mutant RC and equilibration of the energy between P* and the excited state of LHI. The spectrum of the third component in the triple mutant corresponds more closely to the spectrum of the LHI only fluorescence (see Fig. 1), and is probably due to antenna complexes that are not quenched by the reaction centers (Beekman et al., 1994).

In all other investigated mutants and in the wild-type, direct observation of the formation of P* via energy transfer from the antenna is not possible because the lifetime of P* is too short relative to its formation time. For example, in WT RC the primary electron transfer occurs in ~3.5 ps at 294 K and 1 ps at 10 K (Chan et al., 1991; Fleming et al., 1988; Hoff and Deisenhofer, 1997). In the LH(L131) + LHI mutant, electron transfer slows to 12 ps at room temperature and in the HF(L168) + LHI mutant the electron transfer rate constant is the same or slightly faster than in WT RCs at 294 K (Peloquin et al., 1994; Williams et al., 1992). These decay times are too fast to allow significant buildup of P*, which is formed on the 40 ps timescale. This can be seen by analyzing the first decay component of the observed fluorescence decay, which represents energy trapping from LHI to the reaction center (and thus formation of P*) in each of the samples. The first component's lifetime in WT + LHI is 30 ps at 10 K and 42 ps at 294 K, in the mutant HF(L168) + LHI the lifetime is 38 ps at 10 K and 46 ps at 294 K, and in the LH(L131) + LHI mutant the lifetime is 38 ps at all temperatures. This agrees well with previously measured rates of the energy transfer from LHI to the reaction center (Bergstrom et al., 1990; Bergstrom et al., 1989; Woodbury and Bittersmann, 1990). The second decay component, with a lifetime of ~200 ps in WT + LHI and ~250 ps in both single mutants, represents relaxation of a near equilibrium mixture of the states A*, P*, and $P^+H_A^-$, although, it may also be due to the antenna defects as discussed above for LHI-only sample. The third decay, with the lifetime between 680–740 ps in WT + LHI, between 735–820 ps in LH(L131) + LHI mutant, and between 700–855 ps in HF(L168) + LHI mutant, shows further relaxation of the near equilibrium mixture of excited and charge-separated states (see target analysis section). Some of that fluorescence could also be due to the intrinsic LHI fluorescence of antenna complexes unquenched by the reaction centers. The fourth lifetime, between 2.8 ns at 10 K and 6.5 ns at 294 K in WT + LHI, and 3.4 ns at 10 K and 2.7 ns at 294 K in LH(L131) + LHI mutant, most likely corresponds to the decay of the charge separated state $P^+H_A^-$ to the ground state (Tang et al., 1999; Woodbury

and Parson, 1984), which remains in quasi-equilibrium with the antenna excited state. It should also be noted that in the HF(L168) + LHI mutant at low temperatures, kinetics were fitted with only three components. At room temperature, the fourth fluorescence component with a lifetime of 2.6 ns was resolved, and can also be attributed to equilibration between $P^+H_A^-$ and the excited antenna during the $P^+H_A^-$ decay to the ground state. The reason why the fourth component is not observed at low temperatures will be discussed below.

Summarizing, one can see from Figs. 2–6 that the formation of P* via energy transfer can only be directly observed in the double and triple mutants at low temperatures, where the electron transfer slows down significantly and the fluorescence spectra of LHI and RC are better resolved (Woodbury and Allen, 1995). At room temperature in the double and triple mutants, and at all temperatures in the remaining mutants, the P* formation via energy transfer from the antenna is not directly observed because P* decay is too fast for a substantial P* population to build up, and because the A* and P* fluorescence spectra broaden and overlap under these conditions.

The effects of P/P^+ midpoint potential on the nanosecond fluorescence decay component

Another interesting aspect of these results is the observation of different lifetimes and amplitudes for the nanosecond component of the fluorescence decay in the different mutants. This component is associated with the recombination of $P^+H_A^-$ in equilibrium with P* and the LHI excited state (Peloquin et al., 1994; Schenck et al., 1982; Woodbury and Parson, 1984). In isolated reaction centers from the mutants under consideration, the $P^+H_A^-$ recombination time, measured by transient absorbance, is relatively constant (Tang et al., 1999). Therefore, the variability in the fluorescence results is unlikely to be due to variation in the inherent recombination rate of $P^+H_A^-$ to the ground state in the mutant reaction centers themselves. As can be seen from the decay-associated spectra (Figs. 2–6), a nanosecond component was present only in certain mutants and, in some cases, only at certain temperatures. WT + LHI and the LH(L131) + LHI mutant required a nanosecond decay component for a satisfactory fit at all temperatures. In the double and triple mutants, it was not possible to resolve lifetimes longer than a nanosecond in the fitting at any temperature; although in the HF(L168) + LHI mutant this component was resolved only at room temperature.

This can be explained by the changes in the thermodynamics of the system in the different mutants. In HF(L168) + LHI, the mutant with the lowest P/P^+ midpoint potential (410 meV), the energy gap between P* and $P^+H_A^-$ is larger than in WT (Murchison et al., 1993). Accordingly, the population of P* due to $P^+H_A^-$ recombination is smaller compared to WT RCs. This makes the longest fluorescence component essentially undetectable at low temperatures. Even at room temperature, when the probability of thermal repopulation of P* due to $P^+H_A^-$ recombination is much greater, the amplitude of the fourth component is significantly smaller compared to WT + LHI (see Figs. 2 and 4), making the evaluation of the lifetime difficult. In the double and triple mutants, the free energy of the state $P^+H_A^-$ is close to that of P* and A*. Therefore, at room temperature, the rate of the $P^+H_A^-$ recombination can be significantly faster than in isolated reaction centers due to the possibility of decay to the ground state via the antenna excited state. If this decay time speeds up enough, the third and fourth fluorescence decay components become indistinguishable in the fit. This possibility is supported by the fact that the relative amplitude of the third component, in both the double and triple mutants, is larger than the amplitude of the third component in other mutants. At low temperatures, the electron transfer slows down, and the yield of the state $P^+H_A^-$ decreases significantly in these mutants, making the recombination fluorescence on the nanosecond timescale (which is small in any case) difficult to detect (Woodbury et al., 1994; 1995).

Target analysis

Data was also analyzed using target analysis (Ameloot et al., 1986; Holzwarth, 1996). The RC + LHI complex can be described in terms of excited and charge separated states with different standard free energies (see Fig. 7). In the set of RC mutants studied here, the charge-separated state free energies are systematically varied by virtue of the fact that the P/P^+ midpoint potentials are changed in the mutants. At the excitation wavelength used, absorption of light predominantly forms the excited state of the LHI antenna, A*. From this state, the excitation energy is transferred to the initial electron donor of the RC, forming the state P*. From the state P*, electron transfer proceeds forming the charge separated state $P^+H_A^-$. It is likely that after the charge separation, the state $P^+H_A^-$ relaxes in free energy, giving rise to nonexponential decay kinetics of the long-lived fluorescence (Peloquin et al., 1994; Schenck et al., 1982; Woodbury and Parson, 1984). It has been shown that the bacteriopheophytin molecule has at least two conformations, which interconvert on a several hundred-picosecond timescale after initial charge separation (Muh et al., 1998). The relaxation of $P^+H_A^-$ (or conformational changes associated with H_A^- and P^+) can be described using the transitions between two or three thermodynamically distinct $P^+H_A^-$ states. In the model, the rate constants describing the antenna/reaction center system were assigned as follows. The rate constant k_1 represents energy trapping from the LHI antenna to the RC and k_2 represents detrapping. The rate constant k_3 represents the primary electron transfer in the RC and k_4 is the rate constant for charge recombination back to the P*. Rate constants k_5 and k_6 are the forward and backward rate constants that describe an energetic relaxation of $P^+H_A^-$. In some mutants, there is an additional relaxation of $P^+H_A^-$ that has the

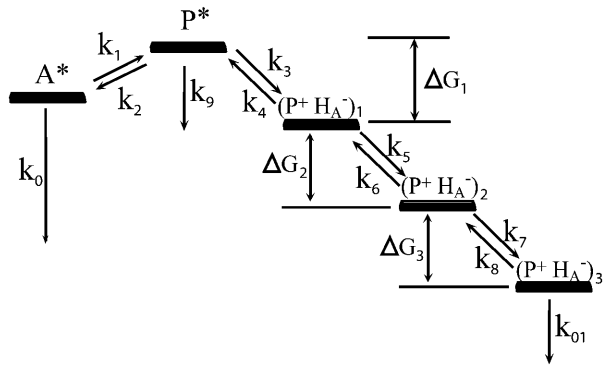

FIGURE 7 State diagram defining the kinetic and thermodynamic parameters used in the target analysis. A*: excited state of LHI, P*: excited state of the RC initial electron donor, $P^+H_A^-$: primary charge separated state of the RC (three different forms are shown denoted with subscripts representing energetically distinct conformations). k_i represent the rate constants between states. ΔG_1 is the standard free energy gap between states P* and $(P^+H_A^-)_1$, ΔG_2 is the standard free energy gap between $(P^+H_A^-)_1$ and $(P^+H_A^-)_2$, and ΔG_3 is the standard free energy gap between the states $(P^+H_A^-)_2$ and $(P^+H_A^-)_3$. It should be noted here that the standard free energy gap between A* and P* is temperature dependent, as there is a significant entropy term due to the larger number of the pigment molecules in the antenna compared to the reaction center.

forward and backward rate constants k_7 and k_8. The rate constant k_{01} describes the recombination to the ground state of the last $P^+H_A^-$ state in the system, either $(P^+H_A^-)_3$ or $(P^+H_A^-)_2$ (the two relaxed forms of $P^+H_A^-$) depending on the RC mutant (see Fig. 7). The rate constant k_0 describes the decay of the excited antenna to the ground state. In some strains, the rate constant k_9 is added to describe the direct decay of P* to the ground state.

Using the kinetic model described above and in Fig. 7, a system of homogeneous linear differential equations was developed to describe the kinetics of energy and electron transfer. This system of equations was solved numerically. For initial conditions, it was assumed that, upon excitation, only the excited state of the antenna is formed, and initial concentrations of all other states are zero. This is a reasonable assumption because there are at least 10 times as many bacteriochlorophyll molecules in the LHI ring as there are in the initial electron donor P. Explicitly taking into account the small initial population of P* (~10%) did not change the fitting results significantly. The parameters used in the fitting were the rate constants shown in Fig. 7 and the wavelength-dependent amplitudes describing the spectral profiles of A* and P* fluorescence. To decrease the number of freely varying rate constants in the system, the decay of the antenna (k_0) was taken to be $(800\ \text{ps})^{-1}$ as determined for the inherent decay time in LHI only mutants (assuming that the quenching process that gives rise to the shorter LHI decay, particularly at room temperature, is not very important compared to quenching by reaction centers). This value for k_0 was then fixed in data fitting for all other mutants. (Releasing this constraint in the WT + LHI strain also resulted in about $(800\ \text{ps})^{-1}$ rate constant for what is likely unconnected antenna decay.) In the mutants with a high P/P^+ midpoint potential, it was necessary to introduce an additional rate constant, k_9, to describe the direct decay of P* to the ground state. In the LH(L131) + LHI and double mutants at low temperature, the rate constant k_9 was fixed to $(200\ \text{ps})^{-1}$ (Breton et al., 1990). The addition of this rate constant in fitting of WT + LHI and HF(L168) + LHI mutant data did not influence the results significantly. The situation for the triple mutant in this respect is discussed below.

The data of WT + LHI and the LH(L131) + LHI mutant were fitted using a model with two excited states (A* and P*) and three charge-separated states ($P^+H_A^-$) at all temperatures. The most noticeable outcome of the analysis was that the trapping from the antenna to the RC was about twofold faster at 10 K than at 294 K: 24 ps vs. 45 ps in WT + LHI and 26 ps vs. 45 ps in the LH(L131) + LHI mutant, respectively (see Table 1). On the other hand, detrapping from the RC to the antenna is somewhat slower at low temperatures than at room temperature: 50 ps (or more) at 10 K and 42 ps at 294 K in WT + LHI and, 40 ps and 24 ps, respectively in the LH(L131) + LHI mutant. This implies that, at low temperatures, there is a change in the relative energetics of the states A* and P*. The free energy between the states A* and P* was calculated using equilibrium constants determined from the forward and backward rate constants. At room temperature, we estimate that A* is lower than P* by ~16–35 meV, which corresponds to previous estimates (Beekman et al., 1994). However, at low temperature, we calculate that P* is nearly degenerate or even lower in energy than A* by almost 1 meV (which is about kT at 10 K). These results are in agreement with the previous hole burning results of the 0–0 transition energies for the reaction centers and LHI antenna (Ratsep et al., 2000). The change in the free energy with temperature is largely due to the entropy term, as LHI antenna contains at least 10-fold more bacteriochlorophylls than P.

The rate constant for initial electron transfer in the reaction center was a free parameter in these fits and the values found agree well with those determined in isolated RCs. For example, in WT RCs, the electron transfer rate at 10 K is found to be 0.9 ps, compared to ~1 ps found in isolated RCs (Chan et al., 1991; Fleming et al., 1988); while at room temperature, 3 ps is the time constant determined by the target analysis, which matches the value found in isolated RCs (Woodbury and Allen, 1995). The electron transfer time constant of 12 ps in LH(L131) mutant RCs has been previously measured only at room temperature (Williams et al., 1992). From our fitting we determined that the electron transfer in LH(L131) + LHI was slower at 10 K (21 ps) than at 294 K (14 ps).

Fluorescence kinetics of the double mutant were fitted with the model based on two excited states and only two charge-separated states (inclusion of the $(P^+H_A^-)_3$ state did not improve the fit). The same general tendencies described

TABLE 1 Results of the fluorescence kinetics fits using target analysis at 10 K, 50 K, 100 K, and 294 K temperatures

Sample	P/P^+ pot, mV	τ_1/τ_2, ps/ps*	τ_3/τ_4, ps/ps	τ_5/τ_6, ps/ns	τ_7/τ_8, ps/ns	τ_{01}, ns	τ_1/τ_2, ps/ps	τ_3/τ_4, ps/ps	τ_5/τ_6, ps/ns	τ_7/τ_8, ps/ns	τ_{01}, ns
		Temperature 10 K					Temperature 50 K				
HF(L168) + LHI	410	22/53	2/24	260/1.2	–	0.79	19/25	5.5/10	194/1.0	–	0.95
WT + LHI	505	24/50	0.9/25	215/1.9	615/46	4.2	22/59	1/14	210/1.6	630/54	3.2
LH(L131) + LHI	585	26/40	21/74	277/2.4	740/42	4.4	30/40	15/90	310/2.3	700/30	3.7
LH(L131) + LH(M160) + LHI	635	40/99	44/39	351/2.5	–	0.73	39/100	45/40	340/4.9	–	0.65
LH(L131) + LH(M160) + FH(M197) + LHI	765	36/1365	–	–	–	–	39/1230	–	–	–	–
		Temperature 100 K					Temperature 294 K				
HF(L168) + LHI	410	37/25	4.5/19	250/1.2	–	0.76	40/10	5.3/45	300/1.0	630/11.0	2.0
WT + LHI	505	32/54	2/18	215/1.5	655/28	4.6	45/24	3/63	225/1.4	770/5.0	5.8
LH(L131) + LHI	585	42/28	5.5/43	320/1.5	780/24	3.4	45/24	14/78	275/1.6	640/13.6	2.3
LH(L131) + LH(M160) + LHI	635	22/38	55/46	350/10.7	–	1.1	50/20	25/100	445/2.0	–	1.0
LH(L131) + LH(M160) + FH(M197) + LHI	765	50/29	–	–	–	–	43/12	–	–	–	–

*The rate constants k_1–k_{01} (see Fig. 7) are presented as lifetimes τ_1, τ_2, τ_3, τ_4, τ_5, τ_6, τ_7, τ_8, and τ_{01} in this table for easier interpretation of the results.

above are observed in this mutant. The energy trapping speeds up from 50 ps at room temperature to 40 ps at 10 K, while detrapping slows down to ~100 ps at 10 K from 20 ps at 294 K. The initial electron transfer time constant also slows down to 34 ps at 10 K from 25 ps at 294 K, which correlates with previous results (Peloquin et al., 1994; Woodbury et al., 1995; Woodbury et al., 1994). Also, the rate constant for the back reaction from $(P^+H_A^-)_1$ to P* is about the same as the forward reaction in the double mutant (see Table 1), which implies that $(P^+H_A^-)_1$ is nearly isoenergetic with P* (see Table 2 in Supplementary Material).

The triple mutant is the most extreme mutant investigated. As mentioned above, its P/P^+ midpoint potential is 260 meV higher than WT. Thus, one might expect that the free energy of the (relaxed) state $P^+H_A^-$ would be almost the same as P* and that early charge-separated states might even be somewhat above P* in free energy. The decay-associated spectra clearly show that there are two distinct populations of fluorescent species, A* and P* (see Fig. 6). We have tried to fit the triple mutant's data with the same model as used for WT and other mutants. However, this did not result in an accurate description of the data, as the χ^2 of the fits was larger than two. Instead, the fluorescence kinetics of the triple mutant were modeled with an altered three-state system consisting only of excited states. In this model, the excited state of the antenna decays to the ground state with the rate constant k_0, or transfers energy to the initial electron donor, P, with the rate constant k_1. Detrapping is described with the rate constant k_2. The states $(P^+H_A^-)_1$ and $(P^+H_A^-)_2$, and $(P^+H_A^-)_3$ were not necessary in the description of the triple mutant fluorescence decay. This is probably a result of both the low quantum yield of the charge separation (10% at 10 K and 50% at 294 K (Peloquin et al., 1994)) and the small free energy gap between the initial charge-separated state and P* (the equilibrium population of P* is so large even after limited charge separation, that it looks more like an excited state than a charge-separated state.) It was necessary, however, to include the decay of P* to a nonfluorescent state in the model. This nonfluorescent state is probably a mixture of a relaxed charge-separated state and the ground state. In addition, for the triple mutant modeling it was necessary to introduce a second, unconnected antenna state, which decayed to the ground state with the same rate constant as the intrinsic decay of the connected antenna population, k_0. Using this model, satisfactory fits were obtained when all rate constants (including k_0, which was fixed for the previous fits) were freely varied. The intrinsic decay rate constant of the excited state of the antenna to the ground state (k_0) was about $(800\ \text{ps})^{-1}$ at low temperatures and $(830\ \text{ps})^{-1}$ at room temperature, in agreement with the LHI only results (see above). The excited state of P had a decay rate constant of $(385\ \text{ps})^{-1}$ at low temperatures and $(240\ \text{ps})^{-1}$ at room temperature. At low temperature, the P* decay rate constant was similar to that found in isolated RCs, $(290\ \text{ps})^{-1}$ (Woodbury et al., 1995), while the room temperature rate constant was four- to fivefold slower than that found for isolated RCs. This may be due to the fact that equilibrium between the initial $P^+H_A^-$ state and P* favors P*. Energy trapping and detrapping follows the same qualitative trend as in other mutants. The trapping slightly speeds up with decreasing temperature, while the detrapping rate constant drastically slows down at 10K; becoming longer than $(1\ \text{ns})^{-1}$ (see Table 1). This, again, implies that the standard free energy of P* is lower than that of A* at low temperatures.

According to the target analysis results, the multiexponential kinetics of the fluorescence decays in mutants, other than the triple mutant, can be explained in terms of the relaxation of the charge-separated state, $P^+H_A^-$, as previously suggested (Peloquin et al., 1994; Schenck et al., 1982; Trissl et al., 2001; Woodbury and Parson, 1984). Some general

trends in the results describing the relaxation of $P^+H_A^-$ can be noted. As one can see from Table 1, the lifetimes describing the relaxations are on the order of a few hundred picoseconds to nearly a nanosecond, which is consistent with the previous results acquired for isolated reaction centers from some of the same mutants (Peloquin et al., 1994). In all cases, the backward time constant for return to the higher energy state is about an order of magnitude smaller than the forward time constant. When the $P^+H_A^-$ state has relaxed to the lowest free energy in the WT + LHI and LH(L131) + LHI mutant (corresponding to the state $(P^+H_A^-)_3$ in Fig. 7), the value of the backward time constant generated by the fit is much longer than the timescale of these measurements (46 ns and 42 ns). On the other hand, the time constants describing the disappearance of the last $P^+H_A^-$ state in the different reaction centers are on the order of several nanoseconds, which coincide with results of single-photon counting fluorescence kinetics measurements of isolated reaction centers (Peloquin et al., 1994).

As noted above, in the case of HF(L168) + LHI and the double mutant, only two $P^+H_A^-$ states were used in the model. The lack of the $(P^+H_A^-)_3$ state does not necessarily mean that this relaxation does not occur. It simply means that the number of parameters required to describe the data accurately for these mutants is less than that needed for WT + LHI. Recall that in both HF(L168) + LHI and the double mutant, only three components were necessary for global fitting. Most likely, the presence of the most relaxed charge-separated state cannot be resolved in our measurements due to a very large free energy gap in the HF(L168) + LHI mutant between P* and $P^+H_A^-$ and the fast $P^+H_A^-$ decay via A* and/or low yield of electron transfer in the double mutant as discussed above. Table 1 shows that the rate constant describing the disappearance of the lowest $P^+H_A^-$ state (k_{01}, see Fig. 7) in the HF(L168) + LHI mutant and the double mutant is faster than that determined for WT + LHI or LH(L131) + LHI. Presumably, this happens for the reasons described above (further relaxation of $P^+H_A^-$ in HF(L168) and decay of $P^+H_A^-$ via A* in the double mutant).

Previously, time-resolved fluorescence and transient absorption measurements have been performed using chromatophores from *Rhodospirillum (Rps.) rubrum* and *Blastochloris (Bl.) viridis* (Bernhardt and Trissl, 2000; Trissl et al., 2001). The authors analyzed their results with a reaction scheme similar to the one presented here. The kinetic rate constants for energy trapping from the antenna to the RC were similar to those reported in Table 1. The authors also found it necessary to introduce relaxation of the charge-separated state, $P^+H_A^-$, by adding a time-dependent free energy gap between P* and $P^+H_A^-$ (Trissl et al., 2001). They estimated that the free energy $P^+H_A^-$ relaxes to ~150 meV below the P*. Our results demonstrate that the free energy of the relaxed state $P^+H_A^-$ in the WT + LHI sample is ~170 meV below P* (see Table 3 in Supplementary materials). The value for the WT + LHI free energy is intermediate between that of Trissl et al., using whole membranes of *Rps. Rubrum*, and Peloquin et al., using time resolved fluorescence of isolated RCs from *Rb. sphaeroides* (Peloquin et al., 1994).

CONCLUSIONS

Increasing the P/P^+ midpoint potential in reaction center mutants and slowing the electron transfer allowed the energy transfer process from the antenna to the RC to be directly resolved at low temperatures. To better understand the complex fluorescence decay kinetics observed, a kinetic model has been developed that describes the fluorescence decays acquired for the all of the mutants at all temperatures measured. Some of the general conclusions obtained from the modeling are:

i. In agreement with earlier work (Peloquin et al., 1994; Schenck et al., 1982; Woodbury and Parson, 1984), the multiexponential decay kinetics of the fluorescence can be described in terms of relaxation of the charge-separated state $P^+H_A^-$.
ii. The energy trapping and detrapping in the reaction centers changes with temperature such that, at room temperature, the detrapping is faster than trapping; indicating a somewhat unfavorable free energy of P* relative to the excited state of LHI. The main reason for this is the entropy of antenna, as suggested by the reversal of the trapping and detrapping rate constants at low temperatures, when the entropy factor diminishes.

SUPPLEMENTARY MATERIAL

An online supplement to this article can be found by visiting BJ online at http://www.biophysj.org/.

Z.K. thanks Dr. Christian Poweleit for help with single-photon counting apparatus, Dr. JoAnn C. Williams and Prof. James P. Allen for providing mutant strains of *Rhodobacter sphaeroides*, and Carole Flores for critical reading of the manuscript.

This research was supported by United States Department of Agriculture grant 98-35306-6396.

REFERENCES

Allen, J. P., and J. C. Williams. 1995. Relationship between the oxidation potential of the bacteriochlorophyll dimer and electron transfer in photosynthetic reaction centers. *J. Bioenerg. Biomembr.* 27:275–283.

Ameloot, M., J. M. Beechem, and L. Brand. 1986. Compartmental modeling of excited state reactions: indentifiability of the rate constants from fluorescence decay surfaces. *Chem. Phys. Lett.* 129:211–219.

Beekman, L. M. P., F. van Mourik, M. R. Jones, H. M. Visser, C. N. Hunter, and R. van Grondelle. 1994. Trapping kinetics in mutants of the photosynthetic purple bacterium *Rhodobacter sphaeroides*: Influence of the charge separation rate and consequences for the rate-limiting step in the light-harvesting process. *Biochemistry.* 33:3143–3147.

Bergstrom, H., C. N. Hunter, R. van Grondelle, and V. Sundstrom. 1990. Energy transfer dynamics in three light harvesting mutants of *Rhodobacter sphaeroides*: a picosecond spectroscopy study. *In* Current Topics in Photosynthesis. Baltscheffsky M., editor. Kluwer Academic Publishers, Dordrecht/ Boston/ London. 173–176.

Bergstrom, H., R. van Grondelle, and V. Sundstrom. 1989. Characterization of excitation energy trapping in photosynthetic purple bacteria at 77 K. *FEBS Lett*. 250:503–508.

Bernhardt, K., and H. W. Trissl. 2000. Escape probability and trapping mechanism in purple bacteria: revisited. *Biochim. Biophys. Acta*. 1457: 1–17.

Breton, J., J.-L. Martin, J.-C. Lambry, S. J. Robles, and D. C. Youvan. 1990. Ground state and femtosecond transient absorption spectroscopy of a mutant of *Rhodobacter capsulatus* which lacks the initial electron acceptor bacteriopheophytin. *In* Reaction Centers of Photosynthetic Bacteria. Michel-Beyerle M.-E., editor. Springer-Verlag, Berlin and Heidelberg. 293–302.

Chan, C.-K., T. J. DiMagno, L. X.-Q. Chen, J. R. Norris, and G. R. Fleming. 1991. Mechanism of the initial charge separation in bacterial photosynthetic reaction centers. *Proc. Natl. Acad. Sci. USA*. 88:11202–11206.

Fleming, G. R., J. L. Martin, and J. Breton. 1988. Rates of primary electron transfer in photosynthetic reaction centers and their mechanistic implications. *Nature*. 333:190–192.

Freiberg, A. 1995. Coupling of antennas to reaction centers. *In* Anoxygenic Photosynthetic Bacteria. Blankenship R.E., M.T. Madigan, and C.E. Bauer, editors. Kluwer Academic Publishers, Dordrecht. 385–398.

Freiberg, A., J. P. Allen, J. C. Williams, and N. W. Woodbury. 1996. Energy trapping and detrapping by wild-type and mutant reaction center of purple non sulfur bacteria. *Photosynth. Res*. 48:309–319.

Frese, R. N., J. D. Olsen, R. Branvall, W. H. J. Westerhuis, C. N. Hunter, and R. van Grondelle. 2000. The long-range supraorganization of the bacterial photosynthetic unit: A key role for PufX. *Proc. Natl. Acad. Sci. USA*. 97:5197–5202.

Gust, D., T. A. Moore, D. K. Luttrull, G. R. Seely, E. Bittersmann, R. V. Bensasson, M. Rougee, E. J. Land, F. C. De Schryver, and M. Van der Auweraer. 1990. Photophysical properties of 2-nitro-5,10,15,20-tetra-p-tolylporphyrins. *Photochem. Photobiol*. 51:419–426.

Hoff, H. J., and J. Deisenhofer. 1997. Photophysics of photosynthesis. Structure and spectroscopy of reaction centers of purple bacteria. *Physics reports*. 287:1–247.

Holzwarth, A. R. 1996. Data analysis of time-resolved measurements. *In* Biophysical Techniques in Photosynthesis. Amesz J., and A. J. Hoff, editors. Kluwer Academic Publishers, Netherlands. 75–92.

Hunter, C. N., H. Bergström, R. van Grondelle, and V. Sundström. 1990. Energy-transfer dynamics in three light-harvesting mutants of *Rhodobacter sphaeroides*: A picosecond spectroscopy study. *Biochemistry*. 29:3203–3207.

Kirmaier, C., and D. Holten. 1987. Primary photochemistry of reaction centers from the photosynthetic purple bacteria. *Photosynth. Res*. 13: 225–260.

Kirmaier, C., and D. Holten. 1993. Electron transfer and charge recombination reactions in wild-type and mutant bacterial reaction centers. *In*. The Photosynthetic Reaction Center. Deisenhofer J., and J. R. Norris, editors. Academic Press, San Diego. 49–70.

Lakowicz, J. R. 1999. Principles of Fluorescence Spectroscopy. Kluwer Academic/Plenum, New York.

Mattioli, T. A., X. Lin, J. P. Allen, and J. C. Williams. 1995. Correlation between multiple hydrogen bonding and alteration of the oxidation potential of the bacteriochlorophyll dimer of reaction center from *Rhodobacter sphaeroides*. *Biochemistry*. 34:6142–6152.

Monshouwer, R., M. Abrahamasson, F. van Mouric, and R. van Grondelle. 1997. Superradiance and exciton delocalization in bacterial photssynthesis ligth-harvesting systems. *J. Phys. Chem. B*. 101:7241–7248.

Muh, F., J. C. Williams, J. P. Allen, and W. Lubitz. 1998. Conformational changes of the photoactive bacteriopheophytin in reaction center from *Rhodobacter sphaeroides*. *Biochemistry*. 998:13066–13074.

Murchison, H. A., R. G. Alden, J. P. Allen, J. M. Peloquin, A. K. W. Taguchi, N. W. Woodbury, and J. C. Williams. 1993. Mutations designed to modify the environment of the primary electron donor of the reaction center from *Rhodobacter sphaeroides*: Phenylalanine to leucine at L167 and histidine to phenylalanine at L168. *Biochemistry*. 32:3498–3505.

Parson, W. W. 1996. Photosynthetic bacterial reaction centres. *In* Protein Electron Transfer. Bendall S.D., editor. BIOS scientific publishers, Oxford. 125–160.

Peloquin, J. M., J. C. Williams, X. Lin, R. G. Alden, A. K. W. Taguchi, J. P. Allen, and N. W. Woodbury. 1994. Time-dependent thermodynamic during early electron transfer in reaction center from *Rhodobacter sphaeroides*. *Biochemistry*. 33:8089–8100.

Ratsep, M., T. W. Johnson, P. R. Chitnis, and G. J. Small. 2000. The red-absorbing chlorophyll a antenna states of photosystem I: A hole-burning study of *Synchocystis* sp. PCC 6803 and its mutants. *J. Phys. Chem. B*. 104:836–847.

Schenck, C. C., R. E. Blankenship, and W. W. Parson. 1982. Radical-pair decay kinetics, triplet yields and delayed fluorescence from bacterial reaction centers. *Biochim. Biophys. Acta*. 680:44–59.

Sundstrom, V., R. van Grondelle, H. Bergstrom, E. Akesson, and T. Gillbro. 1986. Excitation-energy transport in the bacteriochlorophyll antenna systems of *Rhodospirillum rubrum* and *Rhodobacter sphaeroides*, studied by low-intensity picosecond absorption spectroscopy. *Biochim. Biophys. Acta*. 851:431–446.

Tang, C., J. A. Williams, A. K. W. Taguchi, J. P. Allen, and N. W. Woodbury. 1999. $P^+H_A^-$ charge recombination reaction rate constant in *Rhodobacter sphaeroides* reaction centers is independent of the P/P^+ midpoint potential. *Biochemistry*. 38:8794–8799.

Timpmann, K., F. G. Zhang, A. Freiberg, and V. Sundstrom. 1993. Detrapping of excitation energy from the reaction centre in the photosynthetic purple bacterium *Rhodospirillum rubrum*. *Biochim. Biophys. Acta*. 1183:185–193.

Trissl, H. W., K. Bernhardt, and M. Lapin. 2001. Evidence for protein dielectric relaxations in reaction centers associated with the primary charge separation detected from *Rhodospirillum rubrum* chromatophores by combined photovoltage and absorption measurements in the 1–15 ns time range. *Biochemistry*. 40:5290–5298.

van Amerongen, H., L. Valkunas, and R. van Grondelle. 2000. Photosynthetic Excitons. World Scientific Publishing Co., Singapore.

Vermeglio, A., and P. Joliot. 1999. The photosynthetic apparatus of *Rhodobacter sphaeroides*. *Trends Microbiol*. 7:435–440.

Visscher, K. J., H. Bergstrom, V. Sundstrom, C. N. Hunter, and R. van Grondelle. 1989. Temperature dependence of energy transfer from the long wavelength antenna BChl-896 to the reaction center in *Rhodospirillum rubrum*, *Rhodobacter sphaeroides* (w.t. and M21 mutant) from 77 to 177K, studied by picosecond absorbtion spectroscopy. *Photosynth. Res*.:211–217.

Walz, T., S. J. Jamieson, C. M. Bowers, and P. A. Bullough. 1998. Projection structures of three photosynthetic complexes from *Rhodobacter sphaeroides*: LH2 at 6 angstrom LH1 and RC-LH1 at 25 angstrom. *J. Mol. Biol*. 282:833–845.

Williams, J. C., R. G. Alden, H. A. Murchison, J. M. Peloquin, N. M. Woodbury, and J. P. Allen. 1992. Effects of mutations near the bacteriochlorophylls in reaction center from *Rhodobacter sphaeroides*. *Biochemistry*. 31:11029–11037.

Woodbury, N. W., and J. P. Allen. 1995. The pathway, kinetics and thermodynamics of electron transfer in wild-type and mutant reaction centers of purple nonsulfur bacteria. *In* Anoxygenic Photosynthetic Bacteria. Blankenship R.E., M.T. Madigan, and C.E. Bauer, editors. Kluwer Academic Publishers, Dordrecht. 527–557.

Woodbury, N. W., and E. Bittersmann. 1990. Time-resolved measurements of fluorescence from the photosynthetic membranes of *Rhodobacter capsulatus* and *Rhodospirillum rubrum*. *In* Current Research in Photosynthesis. Baltscheffsky M., editor. Kluwer Academic Publishers, Dordrecht. 165–168.

Woodbury, N. W., S. Lin, X. Lin, J. M. Peloquin, A. K. W. Taguchi, J. C. Williams, and J. P. Allen. 1995. The role of reaction center excited state evolution during charge separation in *Rhodobacter sphaeroides* mutant with an initial electron donor midpoint potential 260 mV above wild-type. *Chem. Phys*. 197:405–421.

Woodbury, N. W., and W. W. Parson. 1984. Nanosecond fluorescence from isolated photosynthetic reaction centers of *Rhodopseudomonas sphaeroides*. *Biochim. Biophys. Acta*. 767:345–361.

Woodbury, N. W., J. M. Peloquin, R. G. Alden, X. Lin, S. Lin, A. K. W. Taguchi, J. C. Williams, and J. P. Allen. 1994. Relationship between thermodynamics and mechanism during photoinduced charge separation in reaction center from *Rhodobacter sphaeroides*. *Biochemistry*. 33:8101–8112.

Xiao, X., S. Lin, A. K. W. Taguchi, and N. W. Woodbury. 1994. Femtosecond pump-probe analysis of energy and electron transfer in photosynthetic membranes of *Rhodobacter capsulatus*. *Biochemistry*. 33:8313–8322.

Zhang, F. G., T. Gillbro, R. van Grondelle, and V. Sundstrom. 1992. Dynamics of energy transfer and trapping in the light-harvesting antenna of *Rhodopseudomonas viridis*. *Biophys. J*. 61:694–703.